

## ARTICLES

# Aberrations induced in wavefront-guided laser refractive surgery due to shifts between natural and dilated pupil center locations

Jason Porter, PhD, Geunyoung Yoon, PhD, Diana Lozano, Jessica Wolfing, Remy Tumber, PhD, Scott MacRae, MD, Ian G. Cox, PhD, David R. Williams, PhD

**PURPOSE:** To determine the aberrations induced in wavefront-guided laser refractive surgery due to shifts in pupil center location from when aberrations are measured preoperatively (over a dilated pupil) to when they are corrected surgically (over a natural pupil).

**SETTING:** Center for Visual Science and Department of Ophthalmology, University of Rochester, Rochester, New York, USA.

**METHODS:** Shifts in pupil center were measured between dilated phenylephrine hydrochloride (Neo-Synephrine [2.5%]) and nonpharmacological mesopic conditions in 65 myopic eyes treated with wavefront-guided laser in situ keratomileusis (Technolas 217z, Bausch & Lomb). Each patient's preoperative and 6-month postoperative wave aberrations were measured over the dilated pupil. Aberrations theoretically induced by decentration of a wavefront-guided ablation were calculated and compared with those measured 6 months postoperatively (6.0 mm pupil).

**RESULTS:** The mean magnitude of pupil center shift was  $0.29 \text{ mm} \pm 0.141 \text{ (SD)}$  and usually occurred in the inferonasal direction as the pupil dilated. Depending on the magnitude of shift, the fraction of the higher-order postoperative root-mean-square wavefront error that could be due theoretically to pupil center decentrations was highly variable (mean  $0.26 \pm 0.20 \text{ mm}$ ). There was little correlation between the calculated and 6-month postoperative wavefronts, most likely because pupil center decentrations are only 1 of several potential sources of postoperative aberrations.

**CONCLUSIONS:** Measuring aberrations over a Neo-Synephrine-dilated pupil and treating them over an undilated pupil typically resulted in a shift of the wavefront-guided ablation in the superotemporal direction and an induction of higher-order aberrations. Methods referencing the aberration measurement and treatment with respect to a fixed feature on the eye will reduce the potential for inducing aberrations due to shifts in pupil center.

*J Cataract Refract Surg 2006; 32:21–32 © 2006 ASCRS and ESCRS*

Most eyes receiving conventional laser in situ keratomileusis (LASIK) procedures experience postoperative increases in higher-order aberrations (HOAs).<sup>1–7</sup> The goal of wavefront-guided laser refractive surgery is to remove HOAs as well as correct for sphere and cylinder. However, it is clear from previous studies that HOAs also tend to increase in eyes that have received wavefront-guided LASIK, particularly eyes with low amounts of preoperative HOAs.<sup>8,9</sup> Several mechanisms that could induce these aberrations are currently being investigated.<sup>10–19</sup> One source of induced

postoperative aberrations could be a static offset of a wavefront-guided ablation due to shifts in pupil center location from when aberrations are measured preoperatively over a dilated pupil to when they are surgically corrected over an undilated pupil. It is important to understand the types and magnitudes of aberrations induced by decentered ablations to deliver an optimal customized correction of HOAs.

Laser in situ keratomileusis is typically performed in eyes with pupils in their normal, undilated state under

photopic lighting conditions. This is done for a variety of reasons, including increased patient comfort, the ease with which the surgeon can center a normal, undilated pupil at the beginning of the procedure, and, based on our surgeon's experience, the fact that eye trackers tend to be more robust and reliable when tracking an undilated pupil.

Wave aberration measurements are usually performed in dilated eyes to obtain aberration measurements over pupil sizes that are larger than those experienced in all lighting conditions. Measuring the wave aberration over an undilated pupil could yield a situation in which the wavefront-guided correction was performed over an area smaller than the patient's natural low mesopic or scotopic pupil size. This may lead to an increase in aberrations and a decrease in visual performance when the pupil is large under low-light conditions, such as night driving. Measuring the wavefront over a dilated pupil, however, does not ensure that all the aberrations will be properly corrected during the ablation. Because wavefront-guided LASIK treatments typically use the center of the undilated pupil as a reference point for treating the cornea, any differences in pupil center location between the pharmacologically dilated and normal undilated conditions will result in a static decentration of the wavefront-guided ablation profile on the cornea and the creation of undesired aberrations.

Reports of typical shifts in pupil center location between natural and pharmacologically dilated pupil conditions are relatively sparse and show wide variability.<sup>20-23</sup> Pupil center shifts in different conditions reported in

previous studies are summarized in Table 1. Most investigators found that pupil center location shifted in the superotemporal direction when going from a natural, undilated condition to a pharmacologically dilated condition (cyclopentolate 1%).

The goal of this study was to examine the effect of pupil center shifts on the postoperative wave aberration following wavefront-guided LASIK. We determined the amount of shift in pupil center location between an undilated and dilated pupil state in a group of patients receiving wavefront-guided LASIK ablations. Knowing the patient's preoperative wave aberration and the static difference between the locations of the pupil centers in each condition, we calculated the residual aberrations that would be introduced theoretically due to the measured shifts in an otherwise perfect customized treatment. These theoretically induced aberrations were compared with postoperative wave aberration measurements to assess the relative contribution of these static shifts to the overall amount of HOAs induced after a wavefront-guided LASIK procedure. This study provides some preliminary insights into whether most of the coma induced after wavefront-guided LASIK is a result of a static offset of the ablation due to differences in pupil center location.

## PATIENTS AND METHODS

Sixty-five normal myopic eyes that received wavefront-guided myopic LASIK from the same surgeon were analyzed. Patients with flap complications or patients who received re-treatments were excluded from the study.

A Hartmann-Shack wavefront sensor (Zywave aberrometer, Bausch & Lomb) measured each patient's wave aberration preoperatively and 1 week, 1 month, 3 months, and 6 months postoperatively. The wave aberration was expressed as a Zernike polynomial up to and including 5th-order aberrations according to the standard normalized polynomials and representation established by the VSIA Standards Taskforce.<sup>24</sup> Zernike coefficients are represented using a single  $j$ -index value or a double-index notation, such as  $Z_3^1$  ( $j = 8$ ). A pupil camera internal to the wavefront sensor recorded an image of the eye while simultaneously acquiring the Hartmann-Shack spots. Images were recorded with the room lights off. The illuminance of the stimulus in the Zywave aberrometer was 0.15 lux. The shift in pupil center location was determined from images taken when the pupil was in a natural undilated state and when pharmacologically dilated with phenylephrine hydrochloride (Neo-Synephrine 2.5%). Both preoperative and 6-month postoperative aberrations were measured over the Neo-Synephrine-dilated condition. All aberration measurements are reported for a 6.0 mm pupil. The mean preoperative higher-order root-mean-square (RMS) wavefront error ( $j = 6-20$ ) across all 65 eyes was  $0.46 \mu\text{m} \pm 0.206$  (SD).

Each patient received the wavefront-guided ablation over an undilated pupil using the Technolas 217z laser system. The mean attempted spherical correction was  $-3.12 \pm 1.38$  D and the mean attempted cylinder correction,  $-0.67 \pm 0.50$  D. The wavefront treatment was based on the patient's manifest refraction

Accepted for publication July 11, 2005.

From the Center for Visual Science (Porter, Williams), Department of Ophthalmology (Yoon, MacRae), The Institute of Optics (Wolfe), University of Rochester, Rochester, New York, San Diego State University (Lozano), San Diego, California, Physiological Optics (Tumbar), Schepens Eye Research Institute, Boston, Massachusetts, Bausch & Lomb (Cox), Rochester, New York, USA.

Supported by National Institutes of Health grants EY01319, EY07125, and EY04367 and a research grant from Bausch & Lomb and by the National Science Foundation Science and Technology Center for Adaptive Optics, managed by the University of California at Santa Cruz under cooperative agreement No. AST-9876783.

Drs. Porter, Yoon, MacRae, and Williams have served as consultants to Bausch & Lomb. The University of Rochester has licensed intellectual property to Bausch & Lomb and has a research contract with them. No other author has a financial interest in any product mentioned.

Gary Gagarinas, Brenda Houtenbrink, Gina Crowley, Joseph Stamm, and Steven Schneider provided technical assistance.

Reprint requests to Jason Porter, PhD, Center for Visual Science, University of Rochester, Rochester, New York 14627, USA. E-mail: jporter@cvs.rochester.edu.

**Table 1.** The mean magnitude and direction of the vector shift in pupil center location in different conditions as reported in previous studies.

Condition	Magnitude of Vector Shift (mm)	Direction of Pupil Center Shift	Reference*
Natural undilated pupil			
Photopic to mesopic	0.13 ± 0.07	Temporal	Yang <sup>20</sup>
Photopic to mesopic	~0.10	Inferotemporal	Wyatt <sup>21</sup>
Photopic to scotopic	0.19 ± 0.12	Slight tendency for inferotemporal	Walsh <sup>22</sup>
Natural undilated and dilated pupil			
Mesopic to dilated (cyclopentolate 1%)	0.162 ± 0.083	Superotemporal	Yang <sup>20</sup>
Photopic to dilated (cyclopentolate 1%)	0.183 ± 0.093	Superotemporal	Yang <sup>20</sup>
Photopic to dilated (cyclopentolate 1%)	0.15 ± 0.12	Slight tendency for superotemporal	Walsh <sup>22</sup>

\*First author only

and preoperative wave aberration taken when the eye was pharmacologically dilated with Neo-Synephrine 2.5%. Ablation optical zone sizes ranged between 6.0 mm and 7.0 mm but could not be larger than the patient's maximum pupil size measured by the wavefront sensor. The optical zone was surrounded by a 0.875 mm fixed transition zone. An eye tracker operating at a tracking frequency of 120 Hz monitored and compensated for eye movements.

### Calculating Pupil Center Shifts

Shifts in pupil center location were determined by measuring the center of the undilated and dilated pupils in each patient with respect to the limbus. The limbus served as the reference since it is difficult to perfectly center the pupil on the optical axis of the wavefront sensor and the edge of the limbus does not change with dilation. The pupil camera captured images of each eye in its natural undilated and pharmacologically dilated state. Images were eliminated if eyelashes or part of the eyelid covered any portion of the pupil or a significant portion of the limbus. Each image was analyzed using a custom-written program (Matlab, The MathWorks, Inc). A conventional edge-detection algorithm<sup>25</sup> was applied to detect the edge of the pupil. After a circle was fit to the pupil and the radius and center coordinates were determined,<sup>26,27</sup> the same techniques were used to find the edge, center, and radius of the limbus. The centers of the limbus and the pupil were then known for each image.

Between 1 and 5 preoperative undilated images were obtained for each eye. Each individual image was analyzed once to determine the pupil and limbus center coordinates. The coordinates from all the images analyzed for the same eye were averaged together to obtain mean pupil and limbus center coordinates for each undilated eye. This reduced variability in the relative location between the pupil and limbus centers across images within the same eye. The mean of the standard deviations of the pupil center coordinates was no larger than  $0.44 \pm 0.307 \mu\text{m}$  ( $\pm 95\%$  confidence interval [CI]) in the vertical or horizontal direction and no larger than  $2.60 \pm 0.445 \mu\text{m}$  ( $\pm 95\%$  CI) in the vertical or horizontal directions for the limbus center coordinates.

Each pupil was pharmacologically dilated with Neo-Synephrine 2.5%. On average, the dilated pupil image was captured 40 minutes after instillation of the drug. After full dilation was achieved, the wave aberration was measured and a dilated pupil image was simultaneously acquired. Only 1 wavefront measurement was selected and used to drive the wavefront-guided ablation algorithm for each eye. Therefore, the single dilated pupil

image that was recorded at the same time as the measured wavefront selected for surgery was analyzed. The dilated pupil and limbus center coordinates were calculated 3 times per image and were averaged to obtain a mean set of coordinates for each eye. Analyzing each image 3 times provided an estimate of the Matlab program's repeatability in calculating the pupil and limbus centers. The mean standard deviation of the pupil center coordinates was no larger than  $0.55 \pm 0.657 \mu\text{m}$  ( $\pm 95\%$  CI) in the vertical or horizontal directions and no larger than  $4.26 \pm 1.204 \mu\text{m}$  ( $\pm 95\%$  CI) in the vertical or horizontal direction for the limbus center coordinate. The pupil and limbus coordinates were then known for both the undilated and pharmacologically dilated preoperative pupil conditions in each eye.

As shown in Figure 1, A, the horizontal and vertical distances from the limbus center (white circle) to the dilated pupil center (dark gray circle) were calculated from the dilated pupil image. These distances were added to the limbus center coordinates in the undilated pupil image. Figure 1, B, illustrates where the location of the dilated pupil center would be when superimposed on the undilated image. The difference between the coordinates of the dilated (dark gray circle) and undilated (light gray circle) pupil was calculated to determine the shift in pupil center location. This shift corresponds to a decentration of the wavefront-guided ablation.

### Calculating Theoretically Induced Aberrations

Before calculating the aberrations induced by pupil center shifts, it was important to measure the preoperative wave aberration over a pupil larger than the sum of the desired pupil for reporting the aberrations and twice the magnitude of the pupil shift. This technique ensured that the wavefront-guided correction would extend over the entire pupil being studied. In this study, the desired pupil for reporting aberration results was 6.0 mm. If the maximum dilated preoperative pupil for a given patient was 7.0 mm, the patient would be included in the study only if the magnitude of the shift in pupil center location was less than 0.5 mm. Eyes were eliminated from the study if their pupil center shift was too large to ensure that the wavefront-guided correction would completely overlap the desired pupil.

Knowing the patient's preoperative dilated wave aberration and the difference between the locations of the pupil centers in each condition, we calculated the residual aberrations that would be introduced theoretically due to the measured offsets in an otherwise perfect wavefront-guided treatment. The calculation assumed that decentrations due to shifts in pupil center location

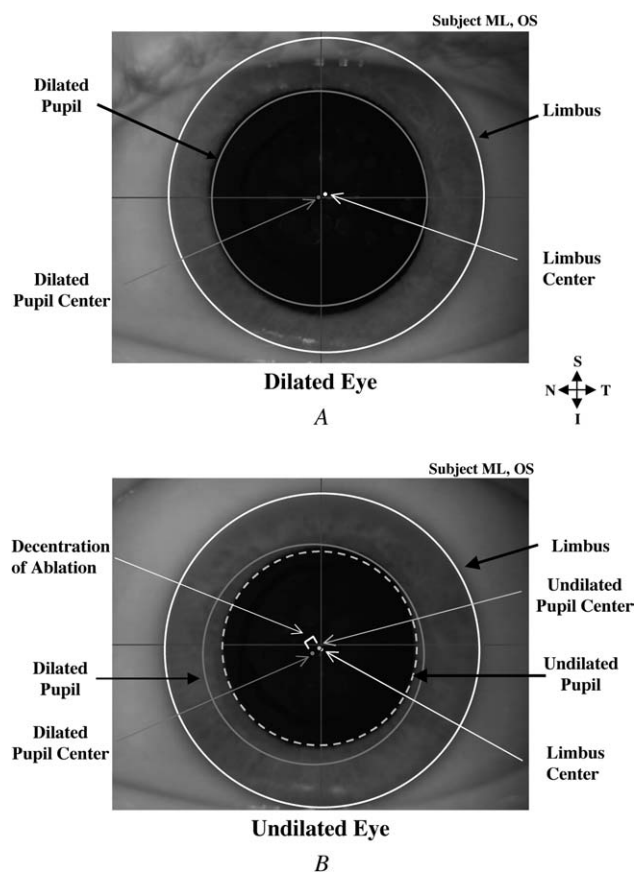


**Figure 1.** Images of the same left eye in (A) a pharmacologically dilated state (Neo-Synephrine 2.5%) and (B) a natural undilated state. The edges of the limbus and dilated pupil are illustrated using solid white and solid dark gray lines, respectively, while that of the undilated pupil is denoted using a dashed light gray line. Limbus, dilated pupil, and undilated pupil centers are represented by white, dark gray, and light gray circles, respectively. A customized ablation in this eye could be decentered due to a slight superotemporal shift from when aberrations were measured over a dilated pupil to when they were corrected over an undilated pupil.

were the only source of error in the wavefront-guided ablation. If there was no difference in pupil center location between a dilated and undilated condition, the desired ablation profile would be perfectly registered and would negate the eye's preoperative wave aberration. This would result in a perfect postoperative correction of the eye's optics with no residual aberrations. However, if there was a difference in pupil center location, the desired correction would be displaced from its intended location and residual aberrations would remain after the treatment. As found by Guirao et al.,<sup>28</sup> decentering a wavefront-guided correction of order  $N$  primarily induces aberrations of order  $(N-1)$ . For example, a wavefront-guided ablation intended to correct for spherical aberration (a 4th-order aberration) would primarily induce coma (a 3rd-order aberration) if the ablation were decentered due to a shift in pupil center.

After these calculations were performed, the theoretically induced aberrations were compared with real aberrations measured 6 months after surgery in each eye. The calculated values were

compared with the postoperative aberrations alone because the patients received a wavefront-guided ablation that should have ideally yielded no postoperative aberrations. Therefore, any aberrations present after the treatment must have been remnants imparted by the procedure.

### Statistical Analysis

Two-tailed  $t$  tests were used to test for significance when comparing the magnitudes of the horizontal and vertical pupil center shifts in all eyes and whether the horizontal and vertical pupil shifts were significantly different between right and left eyes. They were also used to determine significant correlations between the theoretically induced and postoperatively measured aberrations in all 65 eyes. Values of  $P < .05$  were considered significant.

### RESULTS

The mean age of the 65 patients was  $32.60 \pm 8.74$  years. The preoperative myopia was less than  $-7.00$  D (mean  $-3.15 \pm 1.34$  D), and the preoperative cylinder was less than  $-3.00$  D (mean  $-0.56 \pm 0.47$  D).

### Pupil Center Shifts

The mean pupil diameters for the undilated and dilated conditions were  $6.41 \pm 1.19$  mm and  $8.47 \pm 0.72$  mm, respectively. The mean magnitudes and ranges of the horizontal, vertical, and vector shifts in pupil center location between the Neo-Synephrine-dilated and normal undilated conditions are shown in Table 2. The vector shift was calculated as the square root of the sum of the squares of the horizontal and vertical shifts. The mean magnitude for the horizontal shifts in pupil center position ( $0.21 \pm 0.129$  mm) was slightly larger than that in the vertical direction ( $0.18 \pm 0.115$  mm). However, the magnitudes of the shifts in the horizontal direction were not significantly different from those in the vertical direction ( $P = .15$ ). The mean vector shift was  $0.29 \pm 0.141$  mm (range 0.08 mm to 0.64 mm).

The distribution of the magnitudes of the horizontal, vertical, and vector shifts in the location of the pupil center between the pharmacologically dilated and undilated conditions are shown in Figure 2. Most eyes (54% and 63%) experienced less than 0.2 mm of horizontal or vertical shift in pupil center position, respectively. Thirty-one percent of eyes had a vector shift in pupil center location that was less than 0.2 mm, as shown in Figure 2, C. Several eyes experienced large vector shifts, but there was a wide variation in the magnitude of these shifts across eyes.

Pupil center location tended to shift in the inferonasal direction when the pupil went from a natural undilated state to a pharmacologically dilated state. This is illustrated

**Table 2.** Mean and range of magnitudes for horizontal, vertical, and vector shifts in pupil center location between dilated and undilated conditions.

Shift	Mean Magnitude (mm)	Range of Shifts (mm)	
		Minimum Magnitude	Maximum Magnitude
Horizontal	0.21 ± 0.129	0.02	0.51
Vertical	0.18 ± 0.115	0.01	0.46
Vector	0.29 ± 0.141	0.08	0.64

in Figure 3, which shows the shifts in pupil center position in 30 right eyes and 35 left eyes. The center of the undilated pupil in each left and right eye was defined as the origin of the respective plot. The location of each dilated pupil center relative to the undilated pupil center is denoted using diamonds. The means of the horizontal and vertical shifts in pupil center location from an undilated to a dilated state were  $0.16 \pm 0.132$  mm and  $-0.14 \pm 0.161$  mm (right eyes) and  $-0.24 \pm 0.129$  mm and  $-0.17 \pm 0.121$  mm (left eyes), respectively. The right and left eyes had mean vector shifts of  $0.26 \pm 0.142$  mm and  $0.32 \pm 0.138$  mm, respectively. The mean directions of pupil center shift

were along axes oriented at 319 degrees and 216 degrees in the right and left eyes, respectively. There was a significant difference in the horizontal shifts in pupil center location between right and left eyes ( $P = .02$ ). The shifts in the right eyes were negated to account for mirror symmetry between left and right eyes in the horizontal meridian when assessing significance. There was no significant difference in the vertical ( $P = .34$ ) and vector ( $P = .11$ ) shifts between the 2 groups of eyes. Sixty of 65 eyes displayed a pupil center shift in the inferonasal direction as the pupil dilated with Neo-Synephrine 2.5%. Since the wavefront was measured over a dilated pupil but was corrected over an undilated pupil, the wavefront-guided ablation in these eyes would be decentered in the superotemporal direction.

The inferonasal shift in pupil center with dilation was due to the fact that our patients' pupils did not tend to dilate symmetrically about the undilated pupil. Figure 4 shows an example of the change in pupil center location and iris shape from an undilated to a Neo-Synephrine-dilated state in (A) 1 patient's right eye and (B) a different patient's left eye. As seen in the figure, the iris tended to become thinner in the inferonasal direction and was typically thickest in the superotemporal direction after being dilated with Neo-Synephrine.

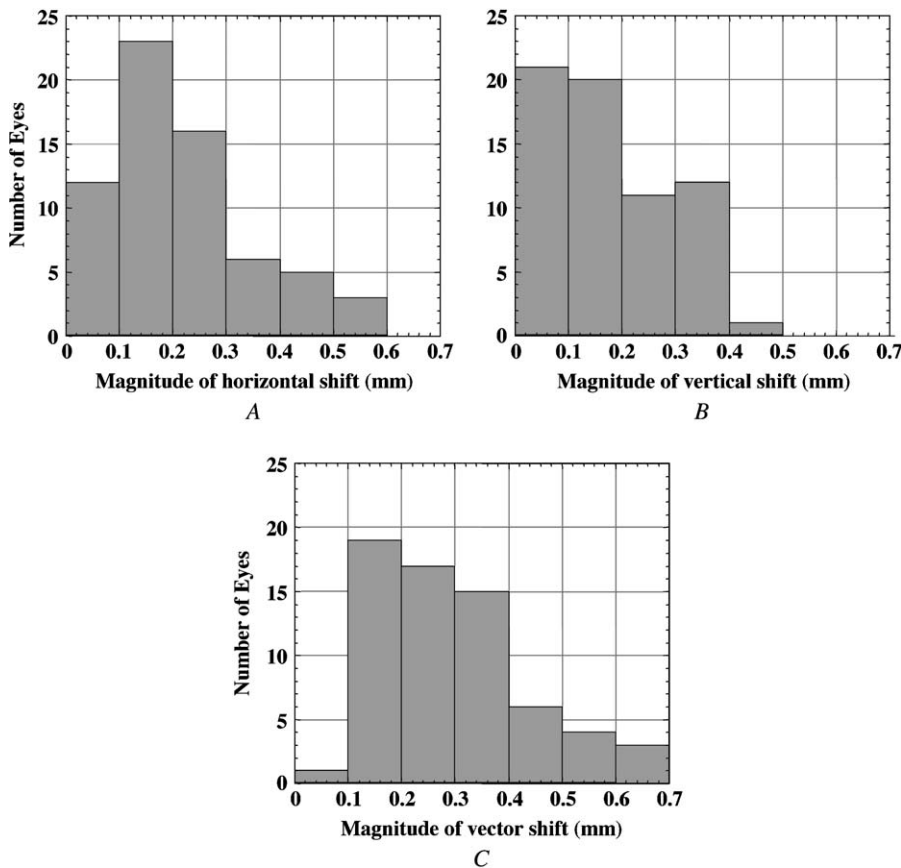


**Figure 2.** Distribution of the magnitude of the (A) horizontal, (B) vertical, and (C) vector shifts in pupil center location between a Neo-Synephrine-dilated and an undilated state in all 65 eyes. The mean horizontal, vertical, and vector magnitudes were  $0.21 \pm 0.129$  mm,  $0.18 \pm 0.115$  mm, and  $0.29 \pm 0.141$  mm, respectively.

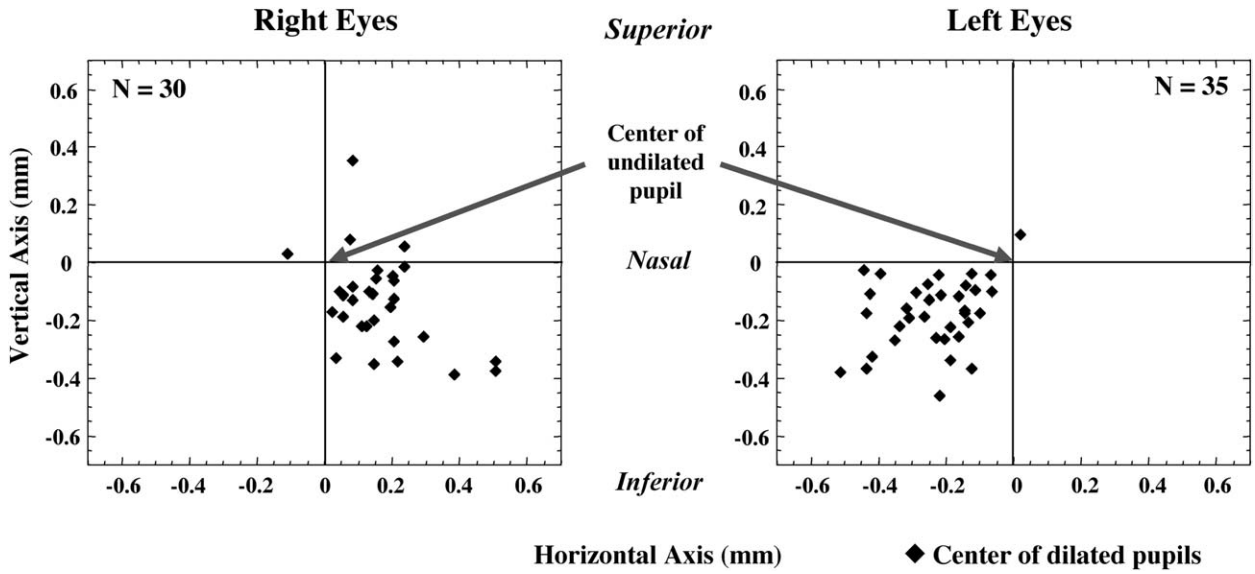


**Figure 3.** Vertical and horizontal shifts in pupil center location from an undilated to dilated state for 30 right eyes and 35 left eyes. The center of the undilated pupil was positioned at the origin of each plot. Diamonds indicate the corresponding centers of all dilated pupils relative to the undilated pupil center position. Pupil center location shifted in the inferior-nasal direction in 60 of 65 eyes when going from a naturally undilated state to a pharmacologically (Neo-Synephrine 2.5%) dilated state. Average horizontal and vertical shifts in the right eyes were  $0.16 \pm 0.132$  mm and  $-0.14 \pm 0.161$  mm, respectively, while the average horizontal and vertical shifts in the left eyes were  $-0.24 \pm 0.129$  mm and  $-0.17 \pm 0.121$  mm, respectively.

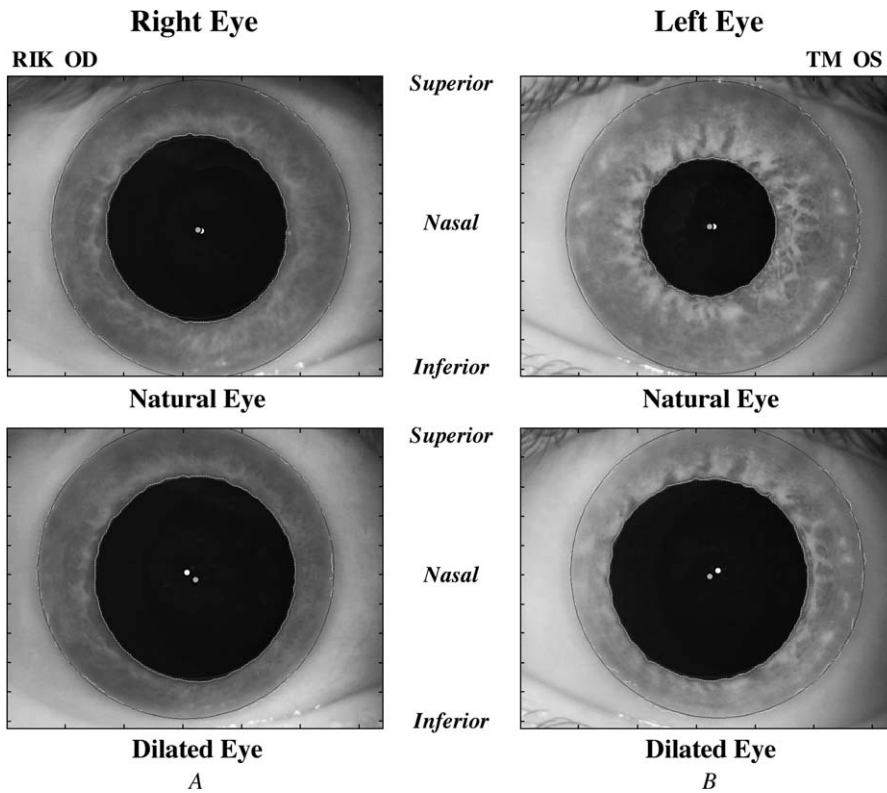


**Figure 4.** Images illustrating the change in pupil center location and iris shape from a natural undilated state to a dilated state in (A) one patient's right eye and (B) a different patient's left eye. Superior, nasal, and inferior directions are noted on the figure. White and gray filled circles denote limbus and pupil centers, respectively. Irises tended to thin more in the inferonasal direction than in the superotemporal direction. Pupil centers tended to shift in the inferonasal direction with dilation.

### Theoretical and Postoperative Aberrations

A wavefront-guided correction was generated for each eye based on the patient's preoperative dilated wave aberration measurement. The correction was decentered by an amount corresponding to the shift in pupil center location from a dilated to a normal, undilated state. The fraction of the measured postoperative higher-order RMS wavefront error that could theoretically be due to shifts in pupil center position was highly variable and depended on the magnitude of the shift. The mean ratio of the theoretically induced higher-order RMS to the actual higher-order RMS measured 6 months postoperatively was  $0.26 \pm 0.202$  (range 0.04 to 1.27).

The distribution of eyes with a given ratio of theoretically induced to 6-month postoperative higher-order RMS for a 6.0 mm pupil is shown in Figure 5. All but 1 eye had a ratio less than 0.76. This indicates that 4% to 76% of the postoperative HOAs could be due to a decentration of the wavefront-guided ablation resulting from a shift in pupil center location. Most eyes had small ratios, with 69% of eyes having a ratio less than 0.3. This implies that postoperative aberrations were typically larger than those theoretically induced due to a pupil center offset of the treatment. The only eye with a ratio larger than 1 (patient RIK\_OD, ratio = 1.27) experienced a substantial decrease in HOAs after wavefront-guided ablation. Patient RIK\_OD had a preoperative higher-order RMS wavefront error of  $1.31 \mu\text{m}$  that was reduced to  $0.84 \mu\text{m}$  6 months

postoperatively. The theoretically predicted higher-order RMS wavefront error based on patient RIK\_OD's large vector pupil shift of 0.63 mm was  $1.07 \mu\text{m}$ .

Figure 5 provides some initial insight into the relative proportion of postoperative aberrations that could be due to offsets of a wavefront-guided ablation. While higher-order RMS wavefront error provides an overall estimate of how aberrated an optical system is, it does not provide direct information on the distribution and magnitudes of the actual aberrations that are present. To better assess the degree of correlation between the theoretical and postoperative aberrations, the correlation coefficients for each Zernike mode between the theoretically induced and 6-month postoperatively measured values in all 65 eyes were calculated, as shown in Table 3. This statistical correlation test was performed on each Zernike mode, and no correction was applied for multiple tests. The signs of all Zernike coefficients that exhibit odd symmetry about the y axis ( $j = 3, 8, 9, 10, 11$ ) were flipped in 1 eye and not the other. Although preoperative wavefronts were measured through 5th-order Zernike modes, 5th-order aberrations were not examined since a decentration of a wavefront-guided correction extending through the 5th order can only produce aberrations of 4th order or lower.

The correlation coefficients for all Zernike modes were weak, indicating that there was a low degree of correlation between the aberrations measured postoperatively and those theoretically calculated after a decentration of a wavefront-guided ablation due to shifts in pupil center location. Defocus ( $j = 4$ ), horizontal coma ( $j = 8$ ), and secondary astigmatism ( $j = 11$ ) were significantly correlated but had very low correlation coefficients ( $R = 0.303$ ,  $R = 0.256$ ,  $R = -0.258$ , respectively). The correlation between the theoretically induced coma terms and the 6-month postoperatively measured counterparts are plotted in Figure 6, as coma is an aberration typically produced when an optical system is decentered. Figure 6, A, shows the poor correlation between the calculated and postoperative values for vertical coma ( $R = -0.077$ ), while Figure 6, B, shows the weak but significant correlation for horizontal coma ( $R = 0.256$ ). The magnitude of the theoretically induced coma terms (square root of the sum of the squares of vertical and horizontal coma) was very weakly correlated with the corresponding postoperatively measured magnitudes ( $R = 0.264$ ), but this low correlation was significant ( $P = .034$ ). When excluding the apparent outlier, denoted as the black circle in Figure 6, C, the correlation negligibly improved to  $R = 0.291$  and was still significant ( $P = .020$ ). In addition, Figure 6, C, illustrates that most eyes had a postoperatively measured coma magnitude that was larger than the magnitude predicted due to offsets of the wavefront-guided ablation caused by shifts in pupil center location. The black line in each plot denotes a perfect correlation

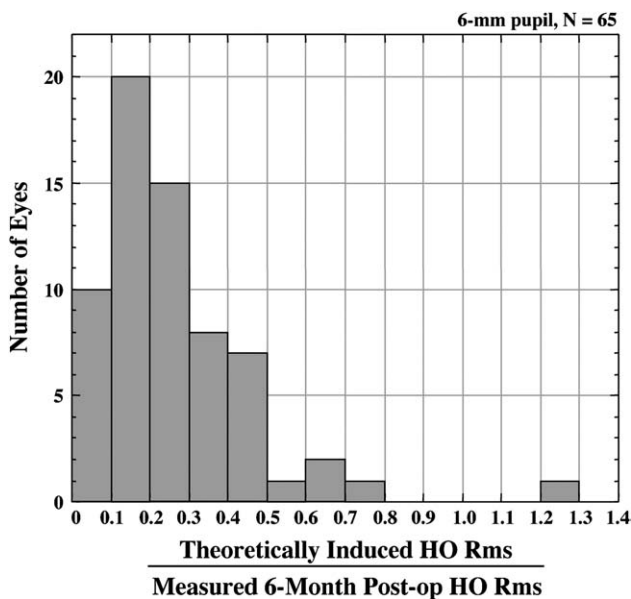


**Figure 5.** Distribution of the ratio of the higher-order (HO) RMS wavefront error theoretically induced solely by shifts in pupil center to the higher-order RMS from 6-month postoperative wavefront sensor measurements in 65 eyes (6.0 mm pupil). The mean ratio was  $0.26 \pm 0.202$ .

**Table 3.** Correlation coefficients for each Zernike mode (up through 4th order) between the theoretically induced and 6-month postoperatively measured aberrations in all 65 eyes and their level of significance.

Zernike Coefficient	Correlation Coefficient, <i>R</i>	95% CI		<i>P</i> value
		Lower	Upper	
<b>j=3</b> ( $Z_2^{-2}$ )	0.123	-0.1248	0.3562	.330
<b>j=4</b> ( $Z_2^0$ )	0.303	0.0640	0.5095	.014*
<b>j=5</b> ( $Z_2^2$ )	0.054	-0.1921	0.2945	.667
<b>j=6</b> ( $Z_3^{-3}$ )	-0.021	-0.2634	0.2244	.870
<b>j=7</b> ( $Z_3^{-1}$ )	-0.077	-0.3151	0.1701	.542
<b>j=8</b> ( $Z_3^1$ )	0.256	0.0123	0.4701	.040*
<b>j=9</b> ( $Z_3^3$ )	0.196	-0.0502	0.4201	.117
<b>j=10</b> ( $Z_4^{-4}$ )	-0.091	-0.3273	0.1569	.473
<b>j=11</b> ( $Z_4^{-2}$ )	-0.258	-0.4721	-0.0149	.038*
<b>j=12</b> ( $Z_4^0$ )	-0.087	-0.3238	0.1607	.493
<b>j=13</b> ( $Z_4^2$ )	0.007	-0.2373	0.2505	.956
<b>j=14</b> ( $Z_4^4$ )	0.163	-0.0846	0.3911	.195

\*Zernike modes that were significantly correlated ( $P < .05$ ).

between the calculated and postoperatively measured aberrations. Sixty-one of 65 eyes were above this line, indicating that their postoperative coma magnitudes were larger than those anticipated from the calculation.

Finally, it could have been possible to obtain low correlation coefficients for individual Zernike modes but, when combined in aggregate, have a theoretically induced wave aberration with a similar overall structure to the postoperative wave aberration. Therefore, a difference wavefront was calculated by subtracting the theoretically induced wave aberration from the postoperative wave aberration in each eye. Second-order through 4th-order ( $j = 3-14$ ) and 3rd-order through 4th-order ( $j = 6-14$ ) RMS values, along with the magnitude of the 2 coma terms, were calculated for the 6-month postoperative and difference wavefronts in each eye. The results are illustrated in Table 4 for a 6.0 mm pupil. If the theoretical aberrations induced due to an ablation offset accounted for a portion of the HOAs, the mean RMS values of the difference wavefronts would be expected to be lower than those of the postoperative aberrations. This was not the case, however, as the mean RMS values of the difference wavefronts were slightly larger than those of the postoperative aberrations in all 3 categories. Both the difference and postoperative RMS values were highly correlated (nearly 1:1 correlation) for the 2nd-order through 4th-order RMS, 3rd-order through 4th-order RMS, and coma magnitudes. This again indicates a poor correlation between the calculated and measured postoperative wavefronts.

## DISCUSSION

The mean vector shift in pupil center location from a mesopic undilated condition to a condition when dilated

with Neo-Synephrine 2.5% was  $0.29 \pm 0.141$  mm in our 65 eyes and occurred in the inferonasal direction with dilation. This mean change was slightly larger and occurred in a different direction than in previously reported studies that used different dilating agents. Most published studies have reported a change in pupil center location between photopic, mesopic, and pharmacologically dilated conditions using cyclopentolate 1%. Walsh<sup>22</sup> found that the location of the pupil center tended to shift slightly temporally (mean  $0.03 \pm 0.15$  mm) and slightly superiorly (mean  $0.02 \pm 0.14$  mm) between a photopic and pharmacologically dilated condition (using cyclopentolate 1%). The mean absolute (or vector) shift was  $0.15 \pm 0.12$  mm. Yang et al.<sup>20</sup> found the position of the pupil center to move a mean of  $0.162 \pm 0.083$  mm in the superotemporal direction from a mesopic to a pharmacologically dilated state using cyclopentolate 1% in 130 eyes. There was also a mean shift in pupil center location of  $0.183 \pm 0.093$  mm in the superotemporal direction when going from a photopic to a pharmacologically dilated pupil state. Wyatt<sup>21</sup> similarly noted a slight tendency for a temporal, but inferior, shift in mean pupil center location of approximately 0.1 mm from a photopic to mesopic condition in 16 eyes. All 3 authors observed large intersubject variability in the degree of shift in pupil center position, with some eyes experiencing shifts of up to 0.6 mm.<sup>20,23</sup> We also found a large range of shifts (between 0.08 mm and 0.64 mm) in our cohort of eyes.

The difference in the direction of the pupil center shift with dilation found in this study compared with those in previous studies could be due to the type of mydriatic used to induce dilation. The eyes in this study received Neo-Synephrine 2.5%, a weaker and different dilating agent than the cyclopentolate 1% used in the studies conducted by Yang et al.<sup>20</sup> and Walsh.<sup>22</sup> As shown in Figure 4, the iris thinned more in the inferonasal direction after being dilated with Neo-Synephrine 2.5% in most eyes, accounting for the inferonasal shift in pupil center location with dilation. Chang et al.<sup>29</sup> found that phenylephrine 2.5% produced an uneven dilation of the pupil, particularly in the vertical direction, while tropicamide 1% yielded a symmetrical dilation.

Dilating agents act on 1 of 2 iris muscles to induce a dilation of the pupil. Cyclopentolate and tropicamide both neutralize the iris' sphincter muscle, which consists of fibers that are arranged in a circular fashion and typically contract uniformly to constrict the pupil. When an appropriate agent inhibits the sphincter fibers, they relax and, as suggested by Chang et al.,<sup>29</sup> collectively move after a short period of time to produce a symmetric dilation of the pupil. Neo-Synephrine, however, acts on the dilator muscle of the iris, which consists of several radiating fiber strands that can contract independently to dilate the iris. A drug that stimulates this muscle in a localized region could produce

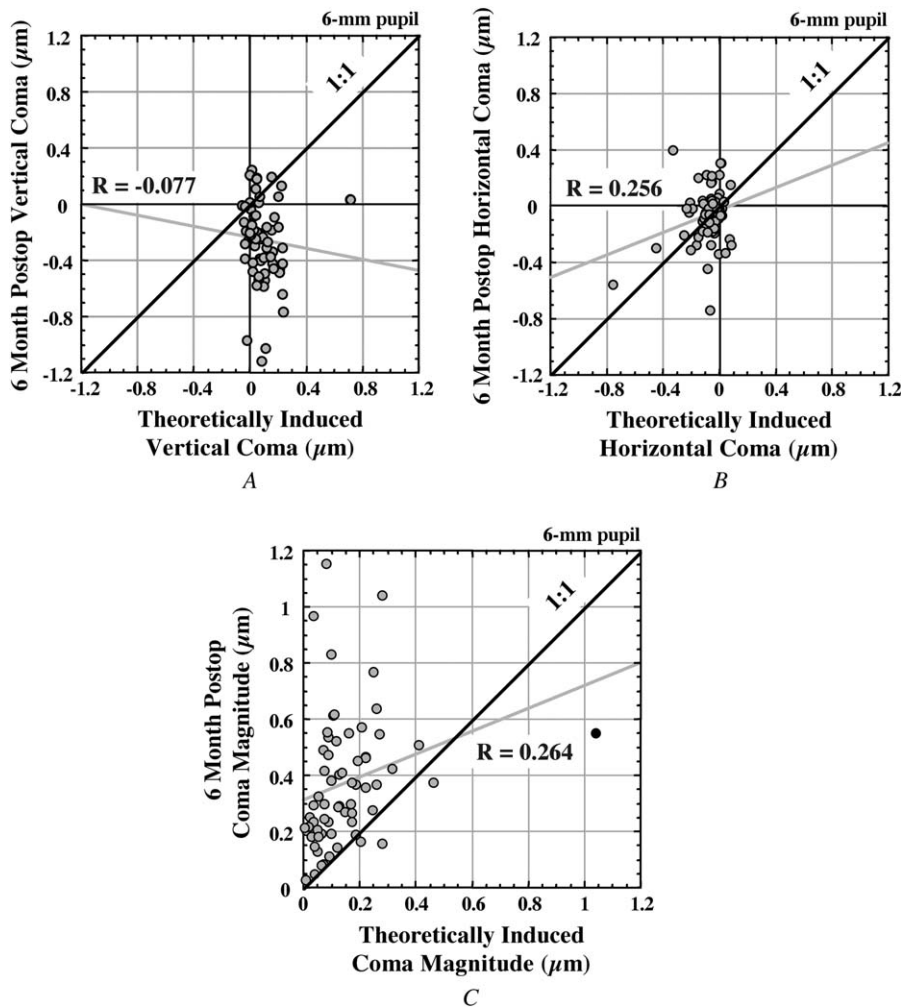


**Figure 6.** Theoretically calculated versus 6-month postoperatively measured (A) vertical coma, (B) horizontal coma, and (C) the magnitude of coma in all 65 eyes (circles) over a 6.0-mm pupil. The black diagonal line has unit slope. A perfect correlation between the theoretically induced and postoperatively measured aberrations exists for points along this line. The gray line is the best-fit line to the data in each plot. There was a significant but low correlation between the calculated and postoperative horizontal coma mode ( $R = 0.256$ ,  $P = .040$ ) and magnitude of the coma modes ( $R = 0.264$ ,  $P = .034$ ).

a nonuniform contraction of the fibers, leading to a non-symmetric dilation. Due to gravity and the fact that tear fluids tend to pool inferiorly, leaving the surface of the eye via canals near the punctum (located nasally and inferiorly in both eyes), it is possible that the dilator muscle fibers could have been stimulated more in the inferonasal portion of the pupil after receiving a drop of Neo-Synephrine. This could explain the nonuniform dilation observed in our eyes with Neo-Synephrine and the shift in pupil center location with dilation in the inferonasal direction.

According to these observed shifts in pupil center location, the wavefront-guided ablations in a majority of our eyes could have been decentered in a superotemporal direction since the wavefront was measured over a pharmacologically dilated pupil but was corrected over an undilated pupil that was relatively constricted due to the bright illumination of the operating microscope. The mean decentration of  $0.29 \pm 0.141$  mm in this study theoretically would result in the induction of HOAs. Based on calculations by Guirao

et al.<sup>28</sup> and Williams et al.,<sup>30</sup> only approximately half the eye's HOAs would be corrected in a wavefront-guided ablation that was statically decentered by 0.3 mm, the mean decentration observed in our study.

The mean ratio of the theoretically induced higher-order RMS error to the 6-month postoperative higher-order RMS error was  $0.26 \pm 0.202$ , implying that, on average, a maximum of 26% of the HOAs after surgery potentially could have resulted from decentrations of a wavefront-guided ablation due to pupil center shifts. However, as illustrated in Tables 3 and 4, there was a weak correlation between the aberrations that were theoretically calculated due to an offset of the ablation and those actually measured 6 months after surgery.

Previous studies that measured aberrations in normal eyes have shown that the mean value of spherical aberration (a 4th-order aberration) in the population is positive and significantly different from zero.<sup>31,32</sup> Therefore, a potential source of the coma (a 3rd-order aberration) induced after

**Table 4.** Average and range of RMS wavefront errors for second order through fourth order, third order through fourth order, and the magnitude of coma for the 6-month postoperatively measured and difference wave aberrations in 65 eyes (6.0-mm pupil).

	Zernike Modes					
	Second Order Through Fourth Order		Third Order Through Fourth Order		Magnitude of Coma	
	Postoperative RMS ( $\mu\text{m}$ )	Difference RMS ( $\mu\text{m}$ )	Postoperative RMS ( $\mu\text{m}$ )	Difference RMS ( $\mu\text{m}$ )	Postoperative RMS ( $\mu\text{m}$ )	Difference RMS ( $\mu\text{m}$ )
Average	1.00 $\pm$ 0.434	1.08 $\pm$ 0.481	0.61 $\pm$ 0.244	0.66 $\pm$ 0.279	0.37 $\pm$ 0.231	0.43 $\pm$ 0.279
Minimum	0.404	0.454	0.219	0.224	0.027	0.024
Maximum	3.101	3.286	1.397	1.475	1.156	1.236
Correlation	$R = 0.955$ ( $P < .0001$ )		$R = 0.961$ ( $P < .0001$ )		$R = 0.945$ ( $P < .0001$ )	

wavefront-guided LASIK could be due to a decentration of the customized ablation that attempted to correct a given amount of spherical aberration or secondary astigmatism.<sup>28</sup> We investigated whether most postoperative coma observed after wavefront-guided LASIK could have resulted from a static offset of the ablation by comparing the values of horizontal and vertical coma (and their magnitude) that would have been induced theoretically with those values measured 6 months postoperatively by the wavefront sensor. There was a small and significant correlation ( $R = 0.256$ ,  $P = .040$ ) between the theoretically calculated and actual postoperative values of horizontal coma in our cohort of 65 eyes. The magnitude of the coma terms was also significantly correlated ( $P = .034$ ), but weakly ( $R = 0.264$ ), between the theoretically predicted and postoperative values. Additionally, Figure 6, C, illustrated that the postoperatively measured magnitudes of the coma modes were larger in 61 of 65 eyes than the magnitudes predicted due to a static offset of the ablation alone. This trend, coupled with the weak correlations observed for the vertical and horizontal coma modes, indicates that there are additional mechanisms responsible for the amount of coma induced after wavefront-guided LASIK.

The low degree of correlation in most of the aberrations was most likely due to the fact that pupil center decentrations are only 1 of several potential sources of postoperative aberrations. The degree of the ablation offset depends on the undilated pupil size of the eye at the time of surgery. It was assumed that the pupil center location during surgery in these undilated eyes was identical to the position measured in an undilated state with the wavefront sensor. However, any patient receiving surgery under light levels different than the mesopic levels used to measure the undilated pupil with the wavefront sensor could have experienced a slightly larger or smaller shift than was actually determined, with the potential for inducing different sets of aberrations.

Any potential changes in the orientation of the wavefront-guided ablation due to cyclotorsional effects were also ignored when calculating the theoretically induced

aberrations. Both the pharmacologically dilated and natural undilated images of the pupil were recorded when the patient was sitting upright at the wavefront sensor. Even though the wavefront measurement is recorded over a dilated pupil when the patient is sitting upright, the surgery is performed when the patient is lying down. Any cyclotorsional rotations that occur when the patient lies down will cause the ablation to be improperly oriented during the surgery.

Taylor and Teiwes<sup>33</sup> noted that cyclotorsional movements were smallest during regular fixation (less than  $\pm 1$  degree) and were largest between an upright and prone position. Thirty-two of 46 eyes had less than 5 degrees of cyclotorsion between the upright and supine conditions. Despite observing cyclotorsional movements of up to 16 degrees, Smith and Talamo<sup>34</sup> reported no significant difference in cyclotorsion between upright and supine positions in 30 eyes for binocular viewing conditions. Becker et al.<sup>35</sup> confirmed these observations and also found no significant positionally induced cyclotorsion between upright, binocular fixation and supine, monocular fixation in 38 eyes. Cyclotorsional movements between these 2 conditions appear to be small and would most likely minimally affect laser refractive surgery outcomes.

In addition, there are several other mechanisms that can affect the postoperative aberration structure of the eye. The flap cut, the flap lift, and the subsequent biomechanical and postoperative healing responses of the cornea have a small role in inducing HOAs in the eye after LASIK.<sup>10-16</sup> Another potential source of HOA induction after LASIK is dynamic eye movements that occur during the ablation. An additional mechanism that could be responsible for the increases in spherical aberration observed after LASIK is the efficiency of a laser pulse when striking different areas of the cornea.<sup>17,19</sup> Inhomogeneities in the cornea, fluctuations in the laser's intensity, and changes in humidity could also yield imperfections in the actual ablation profile applied to the cornea. These mechanisms were not incorporated in our theoretical calculations of the aberrations induced due to a static offset of the ablation and

most likely account for the discrepancies between a majority of the theoretically induced and postoperatively measured aberrations. An important step to achieve an optimal customized correction will be to incorporate all of these separate effects into 1 cohesive model that articulates the overall changes resulting from a LASIK procedure for each individual patient.

In summary, measuring aberrations over a Neo-Synephrine-dilated pupil and treating them over an undilated pupil could result in a shift of the wavefront-guided ablation in the superotemporal direction and an induction of HOAs. There was little correlation between the calculated and 6-month postoperative aberrations when examining the entire wavefront or when looking at individual aberrations. A significant but weak correlation between the theoretically induced and postoperatively measured aberrations seemed to occur for horizontal coma, with a correlation coefficient of 0.256 ( $P = .040$ ). A method that references the aberration measurement and treatment with respect to a fixed feature or set of features will reduce the potential for inducing aberrations due to shifts in pupil center location and torsional errors.

## REFERENCES

- Oshika T, Klyce SD, Applegate RA, et al. Comparison of corneal wavefront aberrations after photorefractive keratectomy and laser in situ keratomileusis. *Am J Ophthalmol* 1999; 127:1-7
- Thibos LN, Hong X. Clinical applications of the Shack-Hartmann aberrometer. *Optom Vis Sci* 1999; 76:817-825
- Williams D, Yoon G-Y, Porter J, et al. Visual benefit of correcting higher order aberrations of the eye. *J Refract Surg* 2000; 16:S554-S559
- Mrochen M, Kaemmerer M, Mierdel P, Seiler T. Increased higher-order optical aberrations after laser refractive surgery; a problem of subclinical decentration. *J Cataract Refract Surg* 2001; 27:362-369
- Endl MJ, Martinez CE, Klyce SD, et al. Effect of larger ablation zone and transition zone on corneal optical aberrations after photorefractive keratectomy. *Arch Ophthalmol* 2001; 119:1159-1164
- Moreno-Barriuso E, Merayo Lloves J, Marcos S, et al. Ocular aberrations before and after myopic corneal refractive surgery: LASIK-induced changes measured with laser ray tracing. *Invest Ophthalmol Vis Sci* 2001; 42:1396-1403
- Marcos S, Barbero S, Llorente L, Merayo-Lloves J. Optical response to LASIK surgery for myopia from total and corneal aberration measurements. *Invest Ophthalmol Vis Sci* 2001; 42:3349-3356
- Mrochen M, Kaemmerer M, Seiler T. Clinical results of wavefront-guided laser in situ keratomileusis 3 months after surgery. *J Cataract Refract Surg* 2001; 27:201-207
- Aizawa D, Shimizu K, Komatsu M, et al. Clinical outcomes of wavefront-guided laser in situ keratomileusis: 6-month follow-up. *J Cataract Refract Surg* 2003; 29:1507-1513
- Pallikaris IG, Kymionis GD, Panagopoulou SI, et al. Induced optical aberrations following formation of a laser in situ keratomileusis flap. *J Cataract Refract Surg* 2002; 28:1737-1741
- Porter J, MacRae S, Yoon G, et al. Separate effects of the microkeratome incision and laser ablation on the eye's wave aberration. *Am J Ophthalmol* 2003; 136:327-337
- Sher NA, Bowers RA, Zabel RW, et al. Clinical use of the 193-nm excimer laser in the treatment of corneal scars. *Arch Ophthalmol* 1991; 109:491-498
- Gartry D, Kerr Muir M, Marshall J. Excimer laser treatment of corneal surface pathology: a laboratory and clinical study. *Br J Ophthalmol* 1991; 75:258-269
- Rogers C, Cohen P, Lawless M. Phototherapeutic keratectomy for Reis Bucklers' corneal dystrophy. *Aust N Z J Ophthalmol* 1993; 21:247-250
- Dupps WJ Jr, Roberts C. Effect of acute biomechanical changes on corneal curvature after photokeratectomy. *J Refract Surg* 2001; 17:658-669
- Roberts C, Dupps WJ Jr. Corneal biomechanics and their role in corneal ablative procedures. In: MacRae SM, Krueger RR, Applegate RA, eds, *Customized Corneal Ablation: the Quest for SuperVision*. Thorofare, NJ, Slack, 2001; 109-131
- Mrochen M, Seiler T. Influence of corneal curvature on calculation of ablation patterns used in photorefractive laser surgery. *J Refract Surg* 2001; 17:S584-S587
- Jiménez JR, Anera RG, del Barco LJ, Hita E. Effect on laser-ablation algorithms of reflection losses and nonnormal incidence on the anterior cornea. *Appl Phys Lett* 2002; 81:1521-1523
- Yoon G, MacRae S, Williams DR, Cox IG. Causes of spherical aberration induced by laser refractive surgery. *J Cataract Refract Surg* 2005; 31:127-135
- Yang Y, Thompson K, Burns SA. Pupil location under mesopic, photopic, and pharmacologically dilated conditions. *Invest Ophthalmol Vis Sci* 2002; 43:2508-2512
- Wyatt HJ. The form of the human pupil. *Vision Res* 1995; 35:2021-2036
- Walsh G. The effect of mydriasis on pupillary centration of the human eye. *Ophthalmic Physiol Opt* 1988; 8:178-182
- Wilson MA, Campbell MCW, Simonet P. Change of pupil centration with change of illumination and pupil size; The Julius F. Neumueller Award in Optics, 1989. *Optom Vis Sci* 1992; 69:129-136
- Thibos LN, Applegate RA, Schwiegerling JT, et al. Standards for reporting the optical aberrations of eyes. In: Lakshminarayanan V, ed, *Vision Science and Its Applications*. Vol. 35 of OSA Trends in Optics and Photonics Series. Washington, D.C., Optical Society of America, 2000; 232-244
- Press WH, Teukolsky SA, Vetterling WT, Flannery BP. *Numerical Recipes in C: The Art of Scientific Computing*, 2nd ed. New York, Cambridge University Press, 1997
- Zahn CT, Roskies RZ. Fourier descriptors for plane close curves. *IEEE Trans Comput* 1972; C-21:269-281
- Granlund GH. Fourier preprocessing for hand print character recognition. *IEEE Trans Comput* 1972; C-21:195-201
- Guirao A, Williams DR, Cox IG. Effect of rotation and translation on the expected benefit of an ideal method to correct the eye's higher-order aberrations. *J Opt Soc Am A Opt Image Sci Vis* 2001; 18:1003-1015
- Chang FW, McCan TA, Hitchcock JR. Sector pupil dilation with phenylephrine and tropicamide. *Am J Optom Physiol Opt* 1985; 62:482-486
- Williams DR, Porter J, Yoon GY, et al. How far can we extend the limits of human vision? In: Krueger RR, Applegate RA, MacRae SM, eds, *Wavefront Customized Visual Correction: the Quest for Super Vision II*. Thorofare, NJ, Slack, 2004; 19-38
- Porter J, Guirao A, Cox IG, Williams DR. Monochromatic aberrations of the human eye in a large population. *J Opt Soc Am A Opt Image Vis Sci* 2001; 18:1793-1803
- Thibos LN, Hong X, Bradley A, Cheng X. Statistical variation of aberration structure and image quality in a normal population of healthy eyes. *J Opt Soc Am A Opt Image Vis Sci* 2002; 19:2329-2348

33. Taylor N, Teiwes W. Eye tracking and alignment in refractive surgery: requirements for customized ablation. In: Krueger RR, Applegate RA, MacRae SM, eds, *Wavefront Customized Visual Correction; the Quest for Super Vision II*. Thorofare, NJ, Slack, 2004 195–202
34. Smith EM Jr, Talamo JH. Cyclotorsion in the seated and supine patient. *J Cataract Refract Surg* 1995; 21:402–403
35. Becker R, Krzizok TH, Wassill H. Use of preoperative assessment of positionally induced cyclotorsion: a video-oculographic study. *Br J Ophthalmol* 2004; 88:417–421